ELSEVIER

Journal of Alloys and Compounds 311 (2000) 137–142

Journal of ALLOYS AND COMPOUNDS

www.elsevier.com/locate/jallcom

Antiferromagnetism in $YbMn_2Ge_2$–Mn magnetic sublattice

M. Hofmann[a,*], S.J. Campbell[b,1], A. Szytula[c]

[a]*Hahn-Meitner-Institut, BENSC, Glienickerstr. 100, D-14109 Berlin, Germany*

[b]*School of Physics, University College, Australian Defence Force Academy, The University of New South Wales, Canberra, ACT 2600, Australia*

[c]*Institute of Physics, Jagellonian University, Krakow, Poland*

Received 15 June 2000; accepted 27 June 2000

Abstract

The magnetic structures of $YbMn_2Ge_2$ with the tetragonal $ThCr_2Si_2$ type structure have been investigated by neutron diffraction measurements over the temperature range ~10–526 K. Rietveld refinements demonstrate that $YbMn_2Ge_2$ has a planar antiferromagnetic structure below T_{N1}~510 K with a canted antiferromagnetic structure below T_{N2}~185 K. The canted antiferromagnetic ground state of $YbMn_2Ge_2$ has a Mn moment value of $\mu_{Mn}(10\ K)=3.03(5)\ \mu_B$, with the *z*-component of the moment $\mu_z(10\ K)=1.72(5)\ \mu_B$, corresponding to a canting angle relative to the *c*-axis of $\theta(10\ K)=55.4(9)°$. No evidence for magnetic ordering of the Yb lattice is obtained although an unusual variation of the *a*-lattice parameter with temperature is observed.

Keywords: Ytterbium manganese germanide; Neutron diffraction; Magnetic structure

1. Introduction

Rare-earth intermetallic compounds containing europium and ytterbium exhibit a wide range of interesting and unusual physical and magnetic properties [1]. This occurs mainly as a result of their mixed valence states (II/III) or changes from one valence state to the other. For example, Eu has a divalent state in $EuMn_2Si_2$ yet a trivalent state in $EuMn_2Ge_2$ [2]. Likewise, YbPdSn exhibits trivalent Yb in the low temperature hexagonal α-phase whereas nearly divalent Yb is obtained in the high temperature orthorhombic β-modification of YbPdSn [3]. Abnormal behaviour of the Yb ion has also been reported for the new ferromagnetic compound $YbMn_6Sn_6$ [4]. The $RT_2Si_{2-x}Ge_x$ compounds (R=Eu, Yb; T=transition metal) of the tetragonal $ThCr_2Si_2$ structure (space group *I4/mmm*) are of particular interest with a range of effects having been reported [2,5–7]. Examples include changes in the Eu valence and Mn magnetic order in $EuMn_2Si_{2-x}Ge_x$ [2] and increase of the effective value of the Yb valence in $YbNi_2(Si_xGe_{1-x})_2$ on compression of the lattice by substitution of Ge for Si and formation of a region ($x = 0.1$–0.9) in which the Yb ions are in the Kondo state [7].

Nowik et al. [8] have recently investigated the magnetic phase transitions in the $YbMn_2Si_{2-x}Ge_x$ series by magnetisation and ^{57}Fe Mössbauer effect studies on ^{57}Fe doped samples. The limiting compound $YbMn_2Si_2$ is consistent with antiferromagnetic order in the Mn magnetic sublattice ($T_N=520$ K) with evidence for a transition at 35 K linked with ordering of the trivalent Yb sublattice. By comparison, $YbMn_2Ge_2$ with divalent Yb ions is reported to reveal several magnetic transitions, the Mn sublattice exhibiting antiferromagnetism below $T_N=495\pm5$ K along with further transitions at ~190, ~350 and ~430 K which were linked to canted spin-reorientation transitions. Given that no neutron diffraction investigations have so far been reported for $YbMn_2Ge_2$, we have carried out an investigation of the magnetic structures of $YbMn_2Ge_2$ over the temperature range ~10–526 K. The Mn magnetic sublattice of $YbMn_2Ge_2$ is found to exhibit planar antiferromagnetism below T_{N1}~510 K with canted antiferromagnetism existing below T_{N2}~185 K.

2. Experimental

The sample was prepared from high purity elements (Yb 99.9%, Mn 99.99% and Ge 99.999%) using an induction

*Corresponding author. Tel.: +49-30-8062-2768; fax: +49-30-8062-2999.

E-mail address: hofmann@hmi.de (M. Hofmann).

[1]Present address: Johannes Gutenberg Universität, D-55128, Mainz, Germany.

0925-8388/00/$ – see front matter
PII: S0925-8388(00)01111-7

furnace under an argon pressure of about 1 bar. The starting materials contained ~10% excess Yb and ~2% excess Mn to compensate for evaporation losses during melting. X-ray and neutron powder diffraction measurements reveal the predominant reflections of the tetragonal 1:2:2 structure as expected, although ~9(2)% of the $YbMn_6Ge_6$ phase is also found to be present (Fig. 1a). $YbMn_6Ge_6$ crystallises in the hexagonal $HfFe_6Ge_6$ structure type and is antiferromagnetic with a Néel temperature of T_N~480 K [9]. A small fraction (<~2%) of the

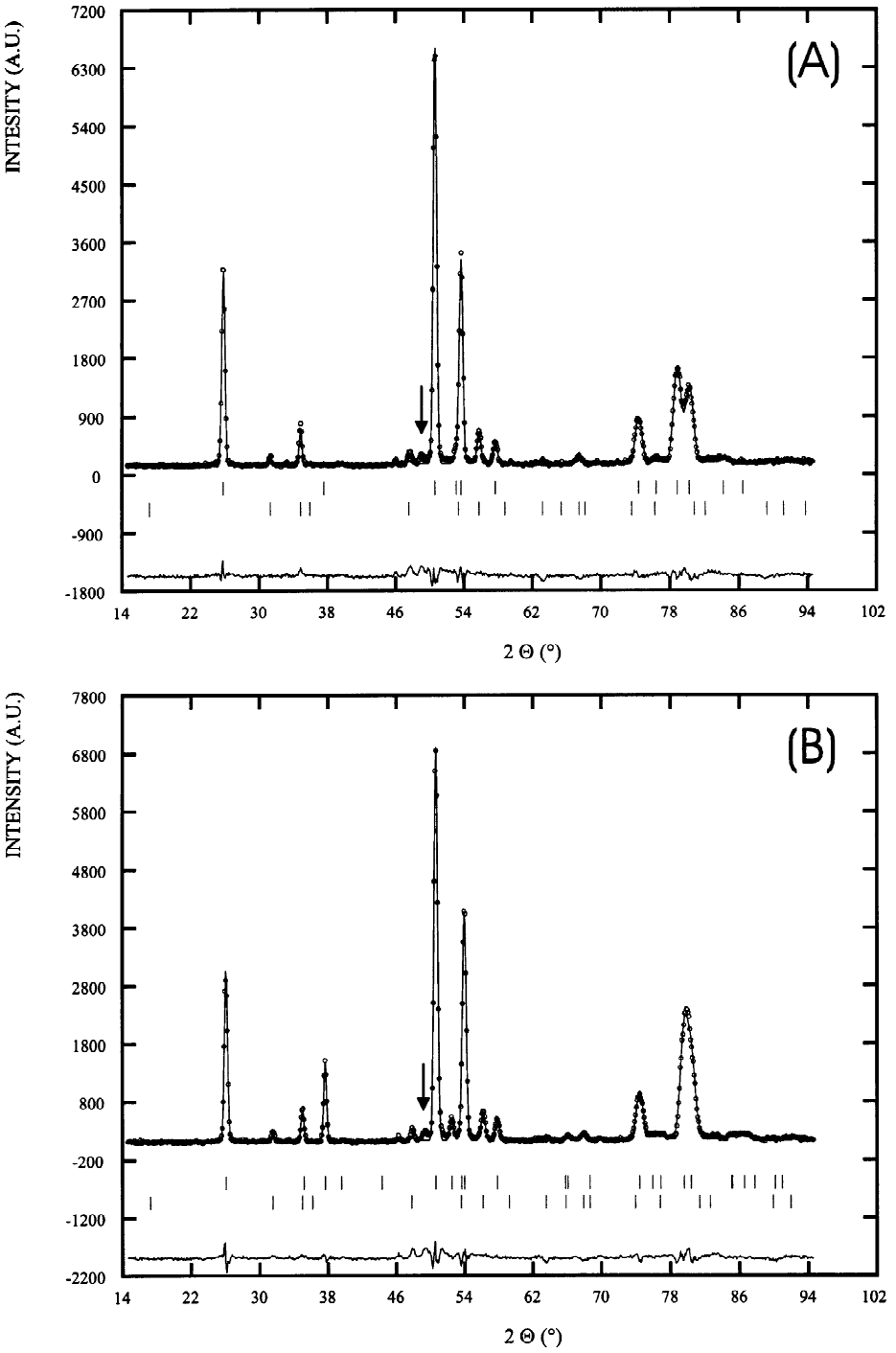

Fig. 1. Rietveld refinements to neutron diffraction patterns of the $YbMn_2Ge_2$ sample at: (a) ~526 K and (b) 10 K. The markers for $YbMn_2Ge_2$ (top) and the impurity $YbMn_6Ge_6$ phase (9(2)%, bottom) are also shown (the main (111) reflection of the Mn_5Ge_3 impurity phase (<~2%) is indicated by an arrow).

Mn_5Ge_3 phase can also be discerned in the diffraction patterns (see the main (111) reflection of Mn_5Ge_3 as indicated by the arrow in Fig. 1). Mn_5Ge_3 is ferromagnetic with a transition temperature of T_C~304 K [10]). As considered recently, preparations of Yb compounds such as YbPtSn [11] and $YbMn_6Sn_6$ [4] with significant fractions of impurity phases are not uncommon.

A comprehensive set of neutron powder diffraction patterns was obtained over the temperature range ~10–526 K on the diffractometer E6 at the Hahn-Meitner-Institut, Berlin (wavelength $\lambda = 2.448$ Å). The variable temperature measurements were carried out with the sample placed in a vanadium can and mounted in a standard cryofurnace. The Rietveld refinements were carried out using the FULLPROF [12] program package which allows simultaneous refinement of the structural and magnetic parameters. Using the coherent scattering lengths for all the elements and the magnetic form factor for Mn as given in Ref. [13], the parameters varied during the initial least square refinements included: a scale factor for each phase, two parameters for the background, the lattice constants and a positional parameter for the Ge atoms in the $YbMn_2Ge_2$ compound. In order to account for preferred orientation effects we fitted an additional correction coefficient [14] for the $YbMn_2Ge_2$ phase to the data in the paramagnetic temperature region: this parameter was then fixed at this optimal value for all other temperatures. Finally the Mn magnetic moment value and an overall temperature factor were refined.

3. Results and Discussion

Fig. 2 shows the neutron diffraction patterns obtained for the $YbMn_2Ge_2$ sample over the temperature range ~10–526 K. Rietveld refinement of the diffraction pattern obtained at ~526 K in the paramagnetic state (Fig. 1a) confirmed that the sample crystallises in the body centred tetragonal space group *I4/mmm* with, as noted above, around 10% of the $YbMn_6Ge_6$ phase also present. As shown in Fig. 3, the initial features revealed by the set of diffraction patterns of Fig. 2 on cooling $YbMn_2Ge_2$ from the paramagnetic region are the onset of magnetic scattering in the (101) and (103) reflections at around T_{N1}~510 K. In common with the behaviour of several compounds in the RMn_2X_2 series (R = rare-earth; X = Si, Ge), the increase in the intensity of the (101) reflection below T_{N1}~510 K marks the onset of antiferromagnetic ordering within the (00*l*) Mn planes [15,16]. This antiferromagnetic contribution is found to persist down to 10 K. In addition,

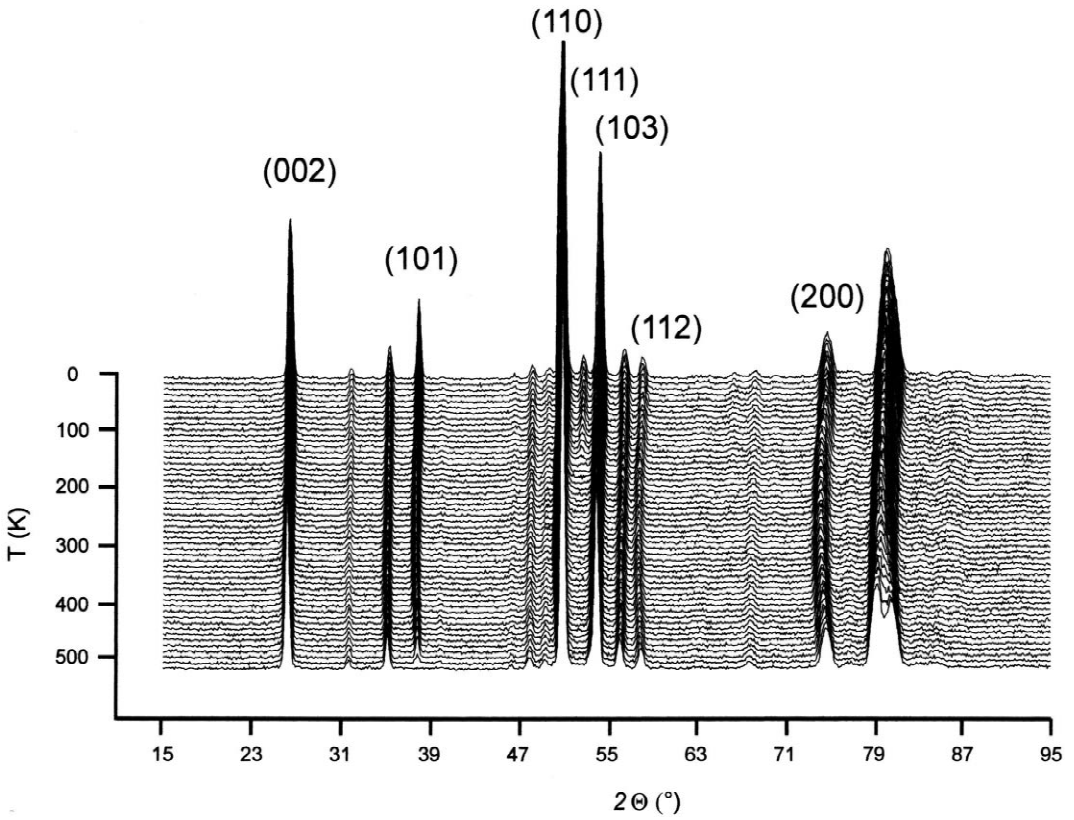

Fig. 2. Neutron diffraction patterns of the $YbMn_2Ge_2$ sample from ~526 K (bottom) to 10 K.

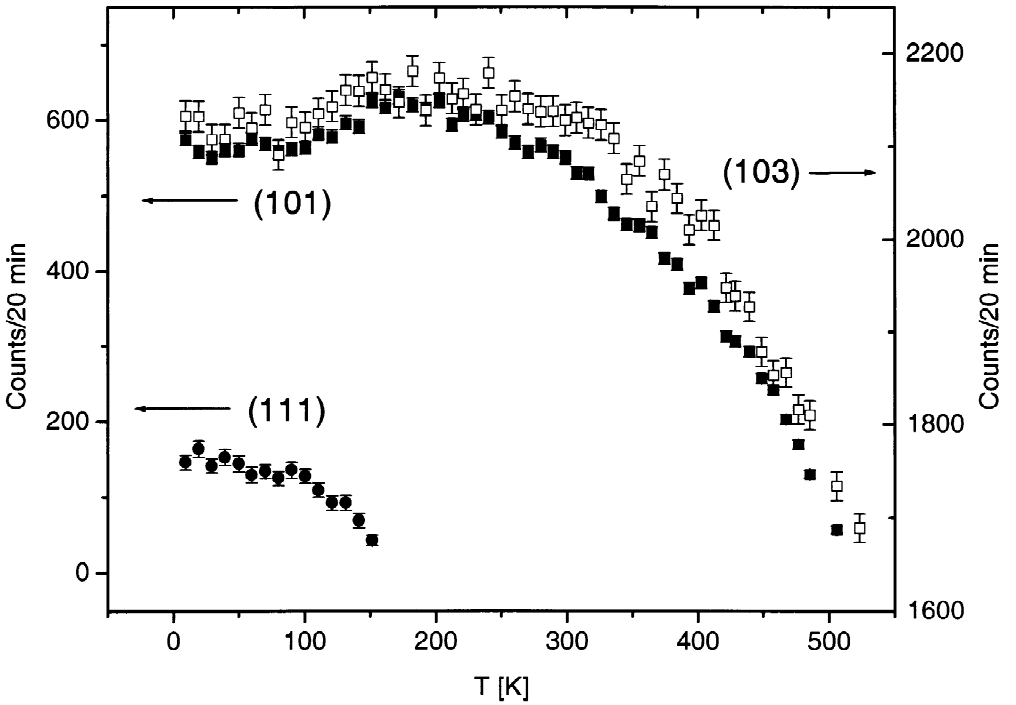

Fig. 3. The variation of the normalised intensities for the (101) (■), (111) (□), and (103) (●) reflections of $YbMn_2Ge_2$ with temperature (cf. Fig. 2).

the intensity ratio for the magnetic contributions of the (101) and (103) peaks indicates that the moments lie in the (00*l*) plane rather than pointing along the *c*-axis, resulting in the layered antiferromagnetism (denoted AF*l* [15,17]) common to many compounds in the RMn_2X_2 series at high temperatures [17,18]. As shown in Figs. 2 and 3, a further magnetic superlattice reflection (111) appears below T_{N2}~185 K. This reflection, of the type $h+k+l=2n+1$, is also of antiferromagnetic origin, and leads to refinement of the neutron diffraction patterns below T_{N2}~185 K based on a canted AF*mc* structure [19,20]. The refinement of the diffraction pattern of the $YbMn_2Ge_2$ sample at 10 K is shown in Fig. 1b with the structural and magnetic parameters of $YbMn_2Ge_2$ at different temperatures given in Table 1 (corresponding to the paramagnetic and the AF*l* and AF*mc* antiferromagnetic phases; see insets to Fig. 4). The onset of the AF*l* phase at T_{N1}~510 K occurs at the intralayer distance of d_{Mn-Mn}~2.861 Å. This temperature is significantly higher than the temperature range over which layered antiferromagnetism is observed in other RMn_2Ge_2 compounds [21], again indicating the distinctive behaviour of Yb compounds. On the other hand, no evidence is obtained for a magnetic contribution to the (112) reflection over the temperature region ~10–526 K (Fig. 2). Calculations show that the (112) reflection is the most sensitive reflection to the onset of ferromagnetism and, within statistical uncertainties, the invariance of the intensity of the (112) reflection over the entire temperature range appears to eliminate the occurrence of a component of ferromagnetic ordering associated with the Mn sublattice in $YbMn_2Ge_2$. However, it is noted that the onset of the AF*mc* phase at T_{N2}~185 K occurs at the intralayer distance d_{Mn-Mn}~2.873 Å. These values more or less overlap the approximate boundary between the AF*mc* and F*mc* phases as reported for other RMn_2Ge_2 compounds [21] and the possibility of a small ferromagnetic component ($<0.4\ \mu_B$) cannot be excluded. Higher resolution neutron diffraction and single crystal magnetisation data are required to clarify this point.

Table 1
Structural and magnetic parameters of $YbMn_2Ge_2$ as determined from Rietveld refinements of neutron diffraction patterns at the temperatures indicated (cf. Figs. 1 and 2), with errors taken from the refinements

Parameter	526 K	250 K	10 K
a (Å)	4.0432(2)	4.0667(2)	4.0420(2)
c (Å)	10.9408(9)	10.8670(9)	10.8363(9)
z (Ge)	0.3863(4)	0.3850(4)	0.3859(5)
μ_x (μ_B)	–	2.55(5)	2.49(5)
μ_z (μ_B)	–	–	1.72(5)
μ_{tot} (μ_B)	–	2.55(5)	3.03(5)
Canting angle (°)	–	90	55.4(9)
R_{wp} (%)	11.2	12.5	12.3
R_{Bragg} (%)	2.3	2.9	1.9
R_{mag} (%)	–	2.3	8.3

The moment values on the Mn sublattice as determined from the refinements to these two antiferromagnetic structures — layered AF*l* for T_{N1}~510 K$<T<T_{N2}$~185 K, and canted AF*mc* for $T_{N2}<$~185 K — are shown in Fig. 4. The Mn moments exhibit a regular monotonic increase with decreasing temperature, as expected, down to T_{N2}~185 K where the moments cant towards the *c*-axis. The overall temperature dependence of μ_{tot}, the total magnetic

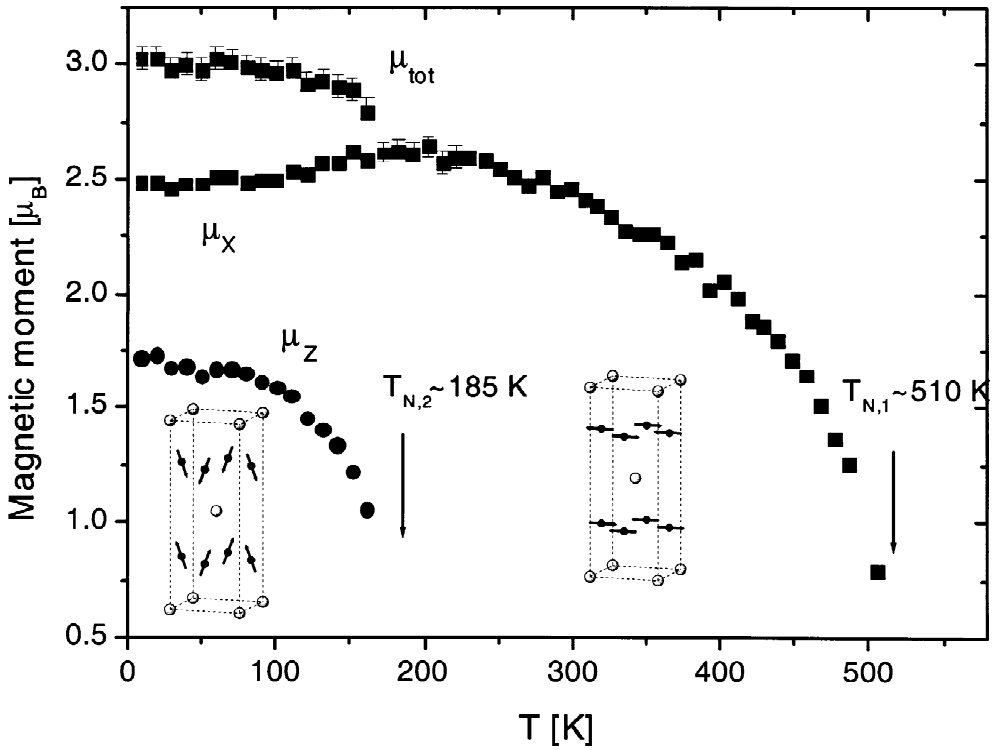

Fig. 4. The temperature dependences of μ_x and μ_y, the components of the magnetic moment on the Mn atoms, and μ_{tot}, the total magnetic moment of $YbMn_2Ge_2$ as determined from Rietveld refinements to the neutron diffraction patterns of Fig. 2. The AF*l* and AF*mc* magnetic structures are shown as insets (see text).

moment on the Mn atoms, is similar to that observed for the magnetic hyperfine field in $YbMn_2Ge_2$ doped with ^{57}Fe [8]. Fig. 5 shows the canting angle, θ, of the Mn magnetic moments with respect to the *c*-axis below T_{N2}~185 K as determined from the present neutron diffraction experiments. Fig. 5 also includes the canting angles for $YbMn_2Ge_2$(^{57}Fe) as deduced by us from the Mössbauer

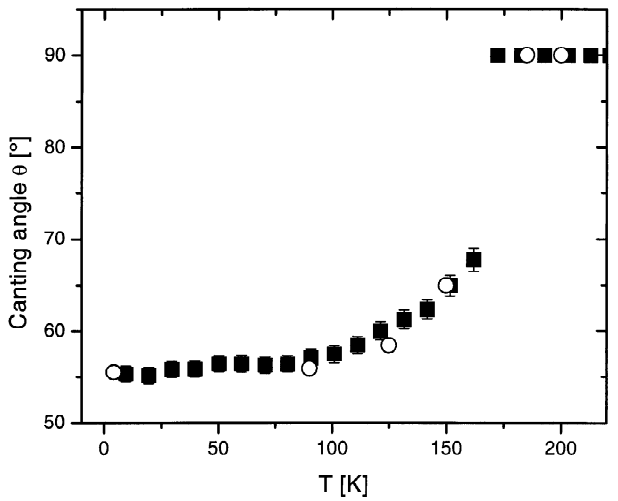

Fig. 5. The canting angle θ relative to the *c*-axis (■), for the Mn magnetic moment in the AF*mc* phase below T_{N2}~185 K. Also shown are the canting angles (○) derived from Mössbauer measurements on ^{57}Fe doped $YbMn_2Ge_2$ [8] as described in the text.

results of Nowik et al. [8]. As discussed previously [17,22], the temperature dependence of the electric quadrupole parameter determined by Mössbauer spectroscopy can be considered in terms of the relative orientation (angle θ) of V_{zz}, the principal component of the electric field gradient (EFG) tensor, and the Mn magnetic moment, and hence the hyperfine magnetic field experienced by the ^{57}Fe nuclei. Given that the principal *z*-axis coincides with the crystallographic *c*-axis and the point symmetry $\bar{4}m2$ of the Mn site axial symmetry, the angular dependent term in the nuclear hamiltonian is $(3\cos^2\theta-1)/2$. Normalising the quadrupole interaction values [8] to the canting angles determined from the present neutron diffraction measurements at T_{N2}~185 K and 10 K, leads to the additional values for the canting angles shown in Fig. 5. Excellent agreement is found between the two sets of θ values which reflect the gradual tipping of the Mn moments out of the crystallographic basal plane with decreasing temperature below T_{N2}~185 K. This agreement demonstrates that for ^{57}Fe-doped $YbMn_2Ge_2$, the observed variation of the quadrupole interaction with temperature below T_{N2}~185 K is due to the changing orientation of the Mn magnetic moment. This behaviour accounts well for the magnetic transition observed at 190(10) K in the earlier magnetisation and Mössbauer measurements on $YbMn_2Ge_2$ [8]. Similar agreement was obtained for the canting angles obtained by neutron diffraction and Mössbauer measurements in the canted ferromagnetic region of ^{57}Fe-doped

$LaMn_2Si_2$ [20,22]. On the other hand, as shown by Fig. 4, no irregularities are observed in the temperature dependence of the Mn moments around 350(10) K and 430(10) K, the temperatures at which additional spin-reorientation transitions were reported for $YbMn_2Ge_2$ [8].

The refinements have also revealed interesting and unusual behaviour for the variation of the lattice parameters with temperature, particularly that of the *a*-lattice constant. The *a*-lattice constant is found to increase as the temperature decreases to around 340 K, followed by a rapid decrease below T_{N2}~185 K. By comparison, the *c*-lattice constant exhibits a more regular behaviour, with a tendency to decrease with decreasing temperature. These effects are reflected in the lattice parameter values given in Table 1 and can also be discerned in the neutron diffraction patterns of Fig. 2 (e.g. the (200) and (002) reflections). This initial expansion of the *a*-lattice parameter below T_{N1}~510 K is probably due to magnetostriction, commensurate with the onset of in-plane antiferromagnetism. On the other hand the sharp decrease of the lattice parameter below ~185 K is thought to be associated with a change in the valence state of Yb. Similar effects — with pronounced anisotropic changes in the *a*-lattice constant — were found in $SmMn_2Ge_2$ and explained in terms of changes in the magnitude of the basal plane magnetic component [23]. Our continuing study of the $YbMn_2Ge_{2-x}Si_x$ system aims to clarify the influence of the Yb valence state on the overall magnetic behaviour of these compounds.

4. Conclusions

In common with other RT_2X_2 compounds with the $ThCr_2Si_2$ structure [17,18], $YbMn_2Ge_2$ has been shown to exhibit a high temperature layered antiferromagnetic structure. $YbMn_2Ge_2$ has a Néel temperature of T_{N1}~510 K and exhibits a transition to canted antiferromagnetism below T_{N2}~185 K, with the canting angle reducing from $\theta = 90°$ to $\theta = 55.4(9)°$ at ~10 K (Fig. 5). Good agreement is obtained with the canting angle derived from Mössbauer effect measurements and between the temperature dependences of the total Mn magnetic moment (Fig. 4) and the ^{57}Fe magnetic hyperfine field on ^{57}Fe-doped $YbMn_2Ge_2$ [8]. No evidence is found for additional spin-reorientation transitions in the Mn sublattice although unusual, anisotropic variation of the lattice parameters with temperature, particularly the *a*-lattice parameter is observed. These features (which are linked with the propensity for mixed valence state of Yb ions) form part of our continuing neutron diffraction investigation of the magnetic behaviour of the $YbMn_2Ge_{2-x}Si_x$ series.

Acknowledgements

SJC acknowledges renewal of an Alexander von Humboldt Research Fellowship while at the Johannes Gutenberg Universität, Mainz. He also acknowledges support from the Access to Major Research Facilities Program, ANSTO.

References

[1] A. Szytula, J. Leciejewicz, Handbook of Crystal Structures and Magnetic Properties of Rare Earth Intermetallics, CRC Press, Boca Raton, 1994.
[2] I. Nowik, I. Felner, E.R. Bauminger, Phys. Rev. 55 (1997) 3033.
[3] R. Kussman, R. Pöttgen, B. Künnen, G. Kotzbya, R. Müllmann, B.D. Mosel et al., Z. Kristallogr. 213 (1998) 356.
[4] T. Mazet, R. Welter, B. Malaman, J. Magn. Magn. Mater. 204 (1999) 11.
[5] B. Chevalier, J.M.D. Coey, B. Lloret, J. Etourneau, J. Phys. C19 (1986) 4521.
[6] H.-J. Hesse, G. Wortmann, Hyperfine Int. 93 (1994) 1499.
[7] E.M. Levin, T. Palewski, B.S. Kuzhel, Physica B 259–261 (1999) 142.
[8] I. Nowik, I. Felner, E.R. Bauminger, J. Magn. Magn. Mater. 185 (1998) 91.
[9] G. Venturini, R. Welter, B. Malaman, J. Alloys Comp. 185 (1992) 99.
[10] J.B. Forysth, P.J. Brown, J. Phys. Condens. Matter 2 (1990) 2713.
[11] R. Pöttgen, A. Lang, R.-D. Hoffmann, B. Künnen, G. Kotzbya, R. Müllmann et al., Z. Kristallogr. 214 (1999) 143.
[12] J. Rodriguez-Carvajal, FULLPROF 98, LLB, 1998.
[13] T. Hahn (Ed.), International Tables for Crystallography, Vol. C, D. Reidel, Dordrecht, 1992.
[14] W.A. Dollase, J. Appl. Cryst. 19 (1986) 267.
[15] G. Venturini, R. Welter, E. Ressouche, B. Malaman, J. Alloys Comp. 210 (1994) 213.
[16] M. Hofmann, S.J. Campbell, S.J. Kennedy, X.L. Zhao, J. Magn. Magn. Mater. 176 (1997) 279.
[17] G. Venturini, R. Welter, E. Ressouche, B. Malaman, J. Magn. Magn. Mater. 150 (1995) 197.
[18] R. Welter, I. Ijjaali, G. Venturini, E. Ressouche, B. Malaman, J. Magn. Magn. Mater. 187 (1998) 278.
[19] I. Ijjaali, G. Venturini, B. Malaman, E. Ressouche, J. Alloys Comp. 266 (1998) 61.
[20] M. Hofmann, S.J. Campbell, S.J. Kennedy, J. Phys. Condens. Matter 12 (2000) 3241.
[21] G. Venturini, B. Malaman, E. Ressouche, J. Alloys Comp. 241 (1996) 135.
[22] S.J. Campbell, J.M. Cadogan, X.L. Zhao, M. Hofmann, H.-S. Li, J. Phys. Condens. Matter 11 (1999) 7835.
[23] G.J. Tomka, C. Kapusta, C. Ritter, P.C. Riedi, R. Cywinski, K.H.J. Buschow et al., Physica B 230–232 (1997) 727.